Available online at www.sciencedirect.com
SCIENCE DIRECT
Nuclear Engineering and Design 235 (2005) 1651–1664
Nuclear Engineering and Design
www.elsevier.com/locate/nucengdes

Supercritical steam cycle for nuclear power plant

Georgi Tsiklauri[a], Robert Talbert[a,*], Bruce Schmitt[a], Gennady Filippov[b], Roald Bogoyavlensky[b], Evgenei Grishanin[b]

[a] *Pacific Northwest National Laboratory, PO Box 999, Richland, WA 99352, USA*
[b] *VNIIAM, Moscow, Russia*

Received 17 January 2004; received in revised form 22 July 2004; accepted 24 November 2004

"Steam is a resource for mankind. It is our challenge and responsibility to further develop and use this resource safely, efficiently and dependably, in an environmentally friendly manner"

Steam 40, Babcock & Wilcox, 1992

1. Background

In ∼200 B.C., a Greek mathematician named Hero invented a simple machine that used steam as a power source. He placed a cauldron of water on a fire until the water boiled and saturated steam at a temperature of ∼100 °C flowed out of the cauldron, a hollow sphere, pivoted at both sides. As the steam escaped, the cauldron through two tubes, which were bent at an angle, the sphere rotated on an axis that passed through the center of the sphere. This sphere was the first steam turbine. Until the late 1800s, steam was used for heat and as a driver in mechanical plants. In the first decade of the 20th century, electrical utility companies were formed. They built steam power stations for electricity generation and distribution, and served residential users across the wide areas of the USA. One of the first stations in the USA was owned by the Commonwealth Edison Company, which used the B&W boilers with steam pressure of approximately 20 bar and a temperature of approximately 290 °C. During the 20th century, the thermodynamic parameters increase dramatically.

In the first three decades, the steam temperature increased from 290 °C to 371 °C and the pressure increased from ∼20 bar to ∼85 bar. The pressure was increased up to the supercritical condition of 310 bar, but later decreased and has stabilized at a level of 240–250 bar. The temperature had been increased up to ∼650 °C, but later decreased to the 540–560 °C level. The historical pressure and temperature curves are presented in Fig. 1.

An important milestone in the generation of electricity occurred in 1957 when the first commercial operation of a thermal power station with a supercritical pressure (SC) of 221.2 bar and a temperature of 621 °C commenced operation in Ohio. Later, supercritical units were widely employed in the power industry of the USA, the former USSR, Germany and Japan.

In 2000, 170 supercritical units were in operation in the US. This is approximately 23% of the entire installed capacity of all fossil-fueled power plants. In Russia, about 30% of the fossil units were supercritical

* Corresponding author. Tel.: +1 509 372 4061; fax: +1 509 372 6421.
E-mail address: bob.talbert@pnl.gov (R. Talbert).

doi:10.1016/j.nucengdes.2004.11.016

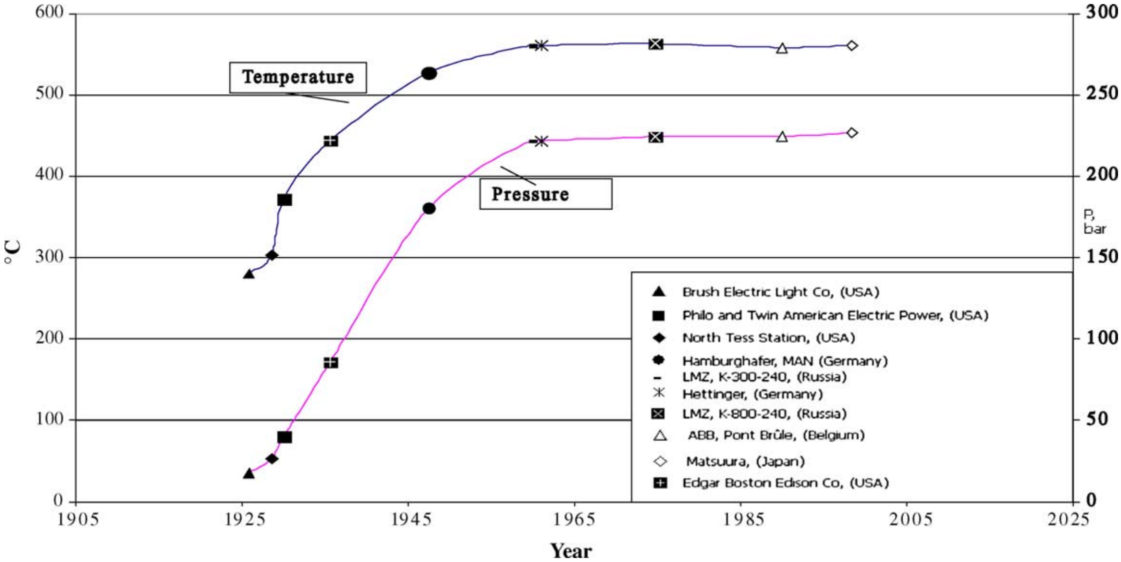

Fig. 1. Increase of thermodynamic parameters of steam cycle for fossil fueled plants.

units, and in Japan, the share of supercritical units of the fossil-fueled installed capacity was about 46%. Supercritical units also constitute about one-fourths of the electrical power plants in Italy and have been employed in Germany and China.

Today, the steam generation systems for electricity production are among the most sophisticated systems designed by mankind. High pressure superheated or supercritical steam is produced in the boiler and is channeled to the turbine generator for production of electricity. The efficiency of supercritical thermal power stations reached a record level of 47–49%. At the present time, the supercritical units are the most reliable, efficient and lowest cost thermal power plants in the world. These plants are mostly fueled by coal. Only the combined cycle gas and steam turbine plants have a higher efficiency (58–60%).

2. Supercritical nuclear reactor (SCR) concept

Both the PWR and BWR Nuclear Power Plants (NPP) are operated on the same thermodynamic principles as fossil-fueled thermal power stations. Both technologies use the Rankine steam cycle; however, the nuclear steam cycle represents a low efficiency cycle with low pressure saturated steam. In spite of improvements in safety and economy, efficiency of the best light water reactor NPPs is very low (34–35%) with CANDU designs being even lower. Comparing the current pressure and temperature of a nuclear steam cycle with the historical data of the pressure and temperature of fossil-fueled plants (Fig. 1), we can conclude that nuclear steam parameters and the thermodynamic efficiency of the current nuclear reactor technology belong to the thermal power technology of the first half of the last century, namely around 1930–1940.

It is generally recognized that raising the steam parameters is the most fundamental and effective way to increase the thermal efficiency and economy of any steam power conversion system. We agree with Professor Y. Oka from Tokyo University that, “the high-temperature supercritical light water reactor is the logical evolution of the LWR. It is based on the experience of LWR design and supercritical fossil-fired power plant technology” (Oka et al., 2003). He proposed a direct cycle supercritical light water reactor with a pressure of 25 MPa, using water as a coolant and moderator. Because of the chemical interaction of water and zirconium at high temperatures, a different material would be required for the cladding. A nickel-based alloy was proposed that should enable one to achieve an average core coolant temperature of 455 °C for upward coolant flow and 508 °C for downward flow. The maximum cladding temperature would reach 620 °C with a steam cycle efficiency of 41% for upward flow and 44% for downward flow. For the design considered by Oka and co-workers (Lee et al., 1999), the safety considerations for the concept, particularly for the beyond-design-basis accidents (BDBA), were the same as for the current nuclear power plants. Further, the supercritical water-cooled reactor design considered by Oka had an estimated core damage frequency approximately equal to that of a standard BWR, and only somewhat higher that for the ABWR (Lee et al., 1999). The proposed design described here enjoys a much lower core damage frequency than the design considered by Oka. The proposed design has a core damage frequency approaching zero.

What are the limiting factors for increasing the steam temperature and pressure to have a more efficient nuclear power plant? The limiting plant component is the current design of the fuel assembly (FA) with rods containing pellets of low-enriched uranium dioxide housed in zirconium cladding. The safety of this type of fuel concept is hobbled by a fast increase of the temperature of the zirconium cladding due to high-temperature heat energy accumulated in the mass of the uranium dioxide pellets, and due to the heat exchange mechanism becoming less efficient due to voiding in the coolant.

The current fuel for U.S. nuclear power plants is designed according to NRC approved criteria. The fuel rod and assembly components are evaluated to ensure that the fuel does not fail under normal operating conditions and in design basis accidents (DBA), such as the loss of coolant accident (LOCA), control rod ejection (drop for BWRs), main steam line break and other DBAs. The most important intrinsic characteristic regarding reactor safety is a negative Doppler reactivity coefficient, which provides instantaneous negative reactivity feedback to any rise in fuel temperature and assures mitigation of reactivity excursions. This characteristic provides rapid termination of prompt critical accidents with additional long-term shutdown capability provided by control rods. Emergency core cooling systems provide a safe core cool-down without damage or fuel failure if a LOCA is encountered.

For beyond design basis accidents, such as a station blackout or anticipated transient without scram (ATWS), the situation is different. For the traditional fuel design, the fast increase of the temperature of zirconium cladding due to high-temperature heat accumulated in uranium dioxide pellets occurs and the fuel will result in severe fuel failure if the accident is not mitigated by recovery (electric power for station blackout and adequate reactivity insertion for ATWS).

To achieve the increased efficiency from a supercritical reactor (SCR), it is necessary to provide fuel cladding that is capable of withstanding the higher temperature encountered in beyond design basis accidents.

The proposed fuel design for a supercritical reactor is to use small spherical particles coated with silicon carbide (SiC). This approach greatly increases the heat transfer area of the fuel and also minimizes the peak central temperature of the fuel, thereby minimizing the latent heat stored in the fuel.

To illustrate the tremendous inherent safety margin provided by this design approach, an analysis of an accident significantly beyond design basis has been performed for both a VVER-1000 reactor and a supercritical reactor using SiC coated particle fuel. The accident chosen was a station blackout simultaneously occurring with an ATWS. The transient temperature curves for traditional fuel (1) and zirconium cladding (2) are shown in Fig. 2.

An analysis of this accident was performed by Filippov and co-workers (Ponamarev-Stepnoy et al., 1999) primarily using the TECH-M code (similar RELAP5/mod3) for thermal hydraulics and the UNK and CONSUL codes for neutronic calculations. For the standard Russian designed VVER-1000, the decrease of core power takes place very slowly; the fuel is heated to a temperature of above 2000 °C. The chain reaction is terminated after approximately 1000 s, when nearly all primary circuit water has been discharged out of core through safety valves. The temperature of zirconium cladding rises and exceeds 1000 °C about 20 s after start of the accident. The onset of a severe steam–zirconium reaction occurs at approximately 700 °C. The probability of core destruction, melting of fuel and release of radioactivity with high dose is very high. A hypothetical accident caused by a terrorist act, destroying the reactor vessel results in similar consequences.

For a supercritical pressure reactor with micro-fuel element (MFE), the fuel temperature in a coated particle fuel element during severe accident (curve (3) in Fig. 2) rises from 600 °C at nominal condition to 800 °C and then after 20 s fall down to coolant temperature. Damage of MFE does not occur. The

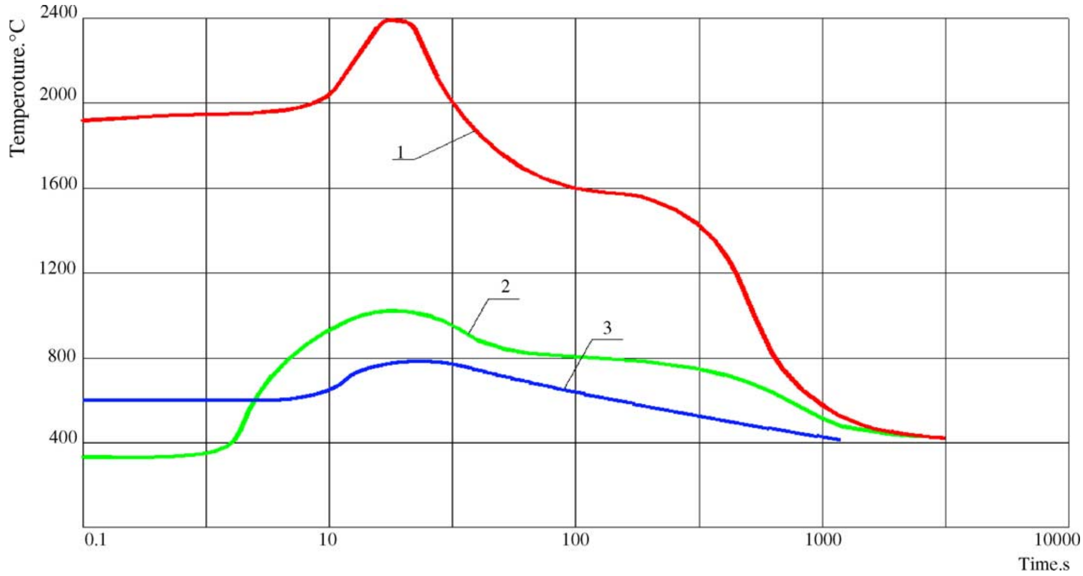

Fig. 2. Accident with total NPP blackout without scram: maximum temperature of fuel (1) and cladding (2) of standard VVER-1000 and (3) temperature of MFE.

acceptable temperature limit for MFE fuel, with SiC as a cladding, is ∼1500 °C (as proven by experiments).

Safety concerns forced the current light water reactors (LWR) to have extensive nuclear reactor safety systems, which provide safe operation and shutdown of nuclear power plants under conditions encountered across a broad spectrum of DBAs. During approximately 40 years of operational history, the safety systems of nuclear power plants have been upgraded in an evolutionary manner. The cost of safety systems, including large containments and core-catchers, has become very high due to the capital cost and long construction periods. These conditions, together with the low efficiency of the steam cycle for the LWR (33–35%), create real financial obstacles to building a new generation of power plants in the US and in Europe.

The SCR provides the potential for cost reduction in both reactor and turbines. It should be noted that the SCR is a smaller reactor, not in power, but in physical size. A once-through core coolant cycle is simpler in design and operation than a re-circulating one. Supercritical water contains higher enthalpy per unit volume than sub-critical water, and as a result, the flow rate is lower. Reactor core, pumps, feedwater reheaters and lines are all smaller than for a standard LWR. The containment is smaller than that of a similar power PWR or BWR due to the reduced reactor thermal power for a given MW_e output, and the primary system contains a lower integrated quantity of stored energy in the coolant and fuel. These are the reasons why the SCR is the smallest in size. The high temperature, supercritical pressure light water reactor is a logical evolution of the LWR. It is based on the experiences of LWR design and safety coupled with supercritical fossil-fired power plant technology. It is the reactor version of the fossil once-through boiler. Its development follows the history of fossil boilers.

3. Supercritical nuclear reactor with micro-fuel elements

Revolutionary improvement of the nuclear plant safety and economy with light water reactors can be reached only with the application of a new fuel; MFE directly cooled by a light water coolant moderator. There are considerable advantages of the MFE as compared with the traditional fuel rods, such as:

- Using supercritical and superheated steam considerably increases the thermal efficiency of the Rankine cycle up to 44–45%.

- Strong negative coolant and void reactivity coefficients with a very short thermal delay time allow the reactor to shutdown quickly in the event of a reactivity or power excursion.
- Core melting and the creation of corium during severe accidents are virtually impossible. The heat transfer surface area is larger by several orders of magnitude due to the small spherical dimensions of the MFE. Further, the small diameter of the fuel spheres significantly lowers the fuel peak central meat temperature, storing much less latent heat in the fuel itself.
- The larger heat exchange surface significantly simplifies residual heat removal by natural convection and radiation from the core to a subsequent passive system of heat removal.
- The fuel assembly walls are made of heat-resistant alloys without zirconium, therefore no steam–zirconium reaction may occur in accidents. There will be no generation of additional heat and explosive hydrogen.
- Large surface area and small thermal flux in the pebble bed do not allow the boiling transition crisis found in traditional PWR and BWR.
- Burnable poison is added lightly and uniformly in the fuel rather than heavily loaded in certain rods. Because of the light uniform loading, less residual will be left in the fuel bundle, improving the reactivity of the bundle late in life.
- The small diameter of the fuel spheres precludes self-shielding, so the fuel sphere depletes uniformly across the diameter, improving fuel economy.
- The thermal neutron absorption of silicon carbide is extremely low, much lower than zirconium. Less parasitic absorption of thermal neutrons takes place in the structure of the fuel and the graphite coating of the fuel provides additional moderation, improving neutron economy.
- Improved neutron economy requires less initial enrichment to achieve end-of-cycle full power reactivity for the same number of full power days of energy harvesting.
- The MFE design ensures the retention of nearly all fission products and fuel within the ceramic cladding.
- It is possible to have continuous or partial re-fueling with MFE during operation to increase the capacity factor.
- The potential cost reduction in reactor, main circulation pumps and turbines are the characteristics of the supercritical reactor. The supercritical steam contains higher enthalpy than sub-critical steam. The total enthalpy drop in the steam turbines is approximately 40% higher and the flow rate per unit of electric power is approximately 60% lower than for a standard BWR.
- A once-through core coolant cycle is simpler in design and operation than the re-circulating one.
- The containment is smaller than that of a BWR. This is due to the high efficiency of the plant, the lower reactor power for a given MW_e output and lower stored thermal energy in the fuel and coolant in the containment.
- Because the SCR has the superheated steam temperature of 550 °C, the steam cycle is simple like for a fossil-fired power plant without an external moisture separator–reheater (MSR). The steam turbine is similar to the large fossil-fired steam turbines with supercritical steam, which have been used worldwide and have had a long and successful operating experience. The supercritical steam turbines achieve the best performance in continuous operation and efficiency.

The conceptual design of the supercritical pressure water reactor of a power 1500 MW_e (SCR-MFE-1500) is depicted in Fig. 3. The thermal power of the reactor is 3390 MW_t with an electrical output of 1520 MW_e net. The core height is 4 m. The core diameter is 3.65 m and the inner diameter of the vessel is in the range of 5 m. The reactor core could contain different numbers of fuel assemblies ranging from 37 to 151 depending upon the dimensions of the fuel assembly. The reactor shares some similar features with a traditional BWR, but control rods are inserted from the top, because the maximum power is at the upper part of the core. Similar to the design of Oka et al. (2003), the vessel wall is cooled by the feed water.

The vessel is made from the conventional steel that is used for PWRs. This approach will avoid the creep of the vessel steel at the supercritical steam temperature. The preliminary analysis used a wall thickness for the cylindrical shell of 38 cm.

The reactor is designed as a once-through reactor. The coolant flow is driven by the main circulation pump without internal reactor re-circulation. An upward

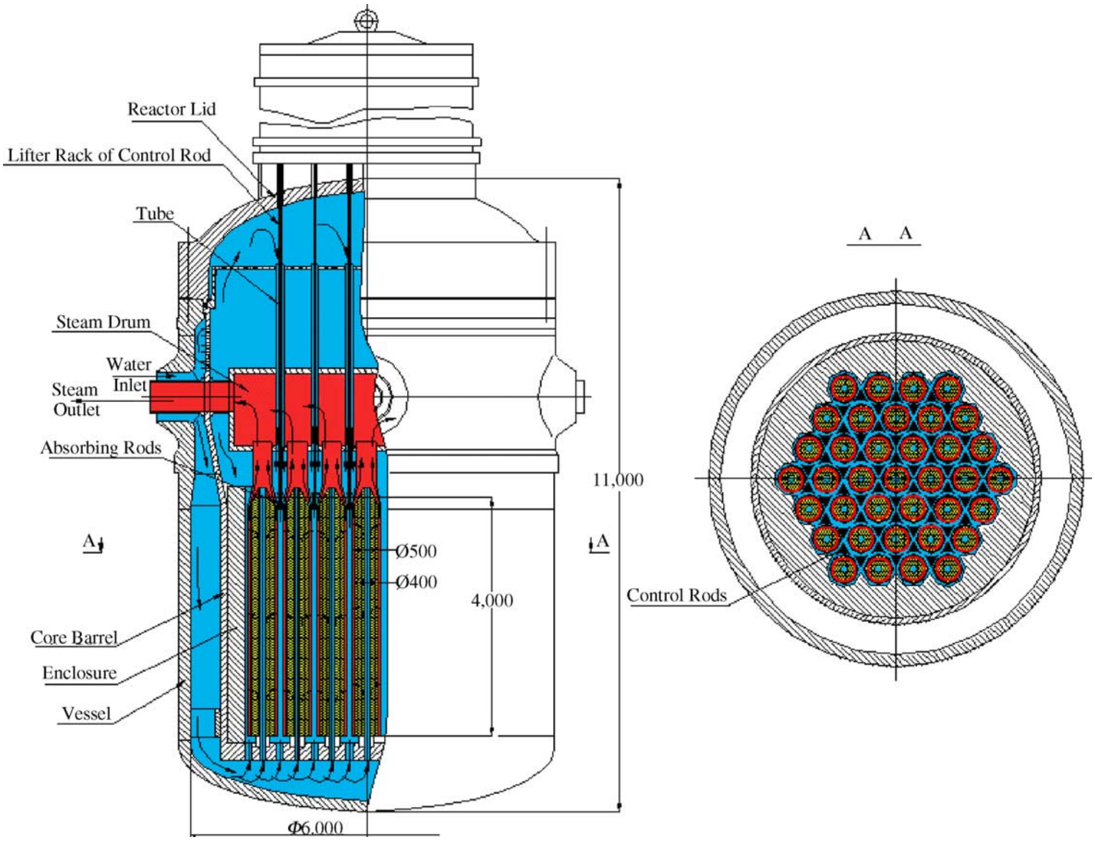

Fig. 3. Supercritical reactor with MFE.

water flow comes from the bottom water plenum into perforated central water channels of the fuel assemblies. The coolant comes through perforations in the wall and penetrates into the micro-fuel element bed in a cross flow direction. The packed bed of micro-fuel particles is located between the central water channel and the outer case, as shown in Fig. 4. The evaporating supercritical water cools the MFE and steam is superheated up to 550 °C at the outlet of the fuel assembly. The superheated and supercritical steam leaves the pebble bed through the perforated outer casing and enters to the steam channel. Steam is then collected in the upper steam header and leaves the reactor through the main steam lines, as shown at Fig. 3. In the upper part of the core, the coolant density significantly decreases (more than in a typical BWR). To compensate for this density decrease, the core space between the fuel assemblies is filled with stagnant feed water, which provides moderation to the upper part of the core.

A spring-loaded upper plate restrains the pebble bed. It is expected that instead of zirconium alloys, the fuel assembly structure can be made of heat-resistant steel or niobium alloy or composite materials with pyrocarbon. Altering the wall perforations can change the profile of the coolant flow along the height of a fuel assembly.

Table 1 compares the calculated parameters of the SCR-MFE-1500 to those of the ABWR. The efficiency of steam cycle for SCR-MFE-1500 is 45.3%, with a net cycle efficiency is 44.75%, 10% higher than the ABWR. The peak SiC cladding temperature is only 50 °C higher than the steam temperature. The temperature limit for SiC clad is 1500 °C so that the safety margin for MFE fuel is very high. The use of supercritical steam provides a significant reduction of the flow rate, ∼20% less than that of the ABWR.

This design uses a MFE arranged in fuel assemblies of special design (hexagonal, square or cylindrical),

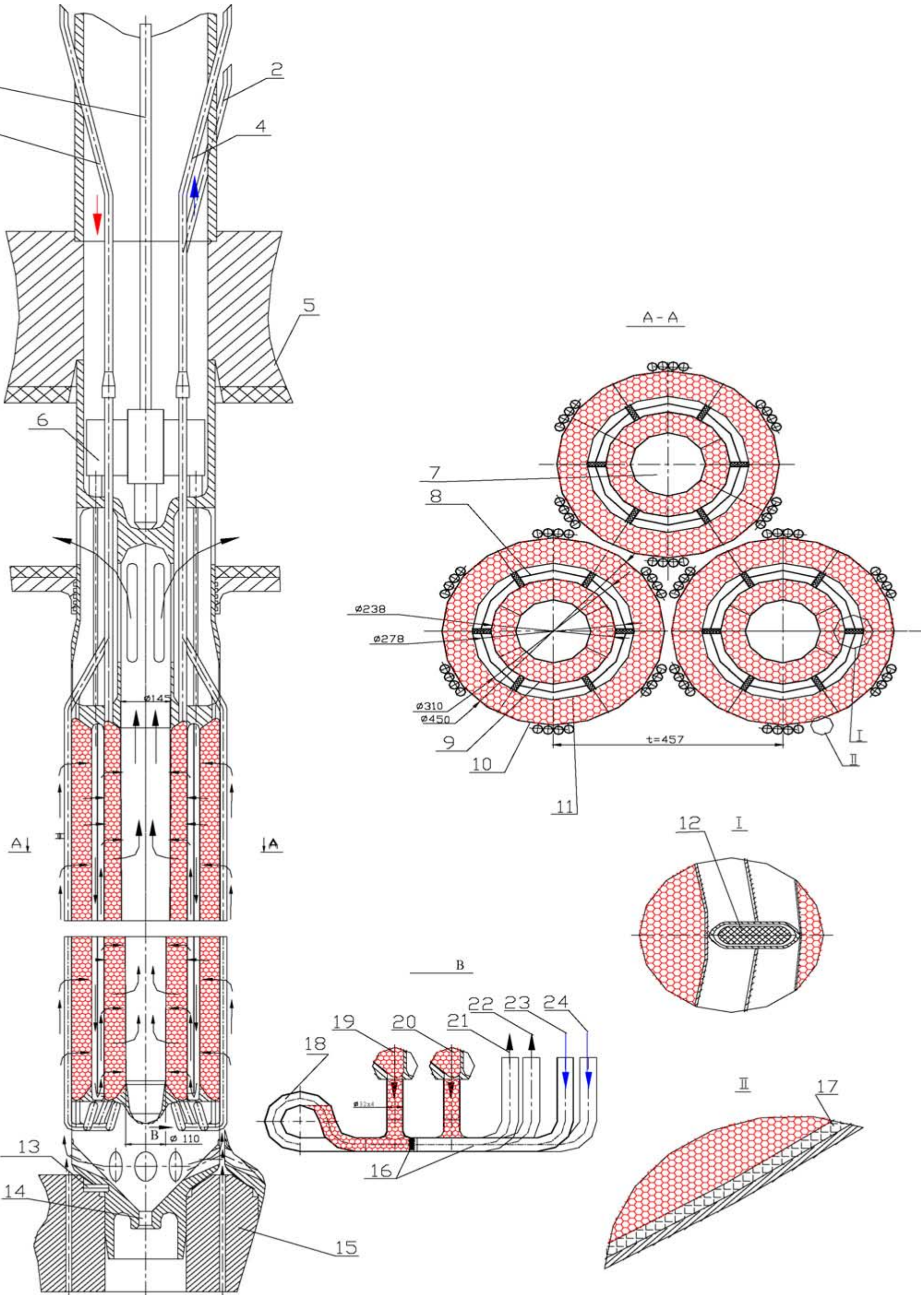

Fig. 4. Design of fuel assembly for continuous re-fueling. (1) tail part, (2) grid, (3) inlet collector, (4) control rod guide tube, (5) particle bed, (6) body, (7) bearing head, (8) lid, (9) spring, (10) stop bushing, (11) stop head, (12) cluster, (13) head part, (14) CP transport pipeline, (15) tube, (16) collector wall, (17) body casing and (18) bushing.

Table 1
Comparison of SCR-MFE-1500 and ABWR

Parameters	SCR-MFE-1500	ABWR
Thermal power (MW_t)	3390	3926
Electrical power (MW_e)	1536	1356
Efficiency (gross) (%)	45.3	34.5
Cladding temperature (average) (°C)	SiC, 470	Zr, 350
Maximum fuel temperature (°C)	750	1300
Steam pressure (MPa)	24	7.17
Steam flow (kg/s)	1680	2118
Average power density (MW_t/m^3)	67.5	50.6
Design burn-up (MWD/kg U)	80	45

which provides for the direct cooling of the MFE by steam–water coolant. The fuel is similar to the TRISO fuel, used for the high-temperature gas reactor (HTGR). The fuel kernel is located in the center of the sphere. The first layer of the MFE coatings is made of pyro-carbon with a density of about 1 g/cm^3. The function of this layer is to provide free volume for the fission gases (mainly Xe and Kr), CO, CO_2 and for the fuel kernel swelling. It also protects the subsequent dense layers from the direct impact of fission products. The buffer layer is coated by a layer of dense pyro-carbon ($\rho \sim 1.8$ g/cm^3). This layer acts as a diffusion barrier for fission products, protects the silicon carbide layer from being contaminated by fuel material in the process of its application, and also provides further protection from the impact of fission products. All dense coatings act as a pressure vessel and as diffusion barriers. The protective layer of silicon carbide acts as a main diffusion and load-bearing barrier that prevents the fission products from being released to the coolant.

Heat-resistant austenitic stainless steel of H18N10T type is considered as the structural material for the fuel assembly casing. According to the evaluation performed, this steel provides for preservation of fuel assembly shape up to the temperature of ∼1100 °C. Outlined is a technical feature that can provide for the preservation of fuel assembly shape up to the temperature of ∼1500 °C. This is most probably achievable with the use of Nb10%Cr10%Al-type alloys.

The online (periodical) re-fueling is an advantage of the MFE fuel assembly. The design scheme of the fuel assembly for the system of online re-fueling is shown in Fig. 4. It is different due to the presence of a pipe (detail 14) in the fuel assembly head part that is necessary to supply the MFEs to the particle-bed, and also by the presence of a conical part of the particle-bed at the bottom of the fuel assembly. This conical piece is ended by a pipe (detail 14) for the discharge of spent MFEs from the core.

4. Reactor safety

During full power operations, the peak fuel temperature in the center of the 2-mm diameter MFE is 750 °C. Furthermore, its thermal delay period for temperature equilibration between fuel and coolant is about 0.014 s. Thus, during any transient (about 2–50 s), the fuel temperature practically follows the coolant temperature. The reactor safety characteristics result from the strong negative temperature and void reactivity coefficients and the low thermal lag time for the coolant temperature response to increases in the fuel temperature. These characteristics allow the SCR-MFE-1500 to shut itself down rapidly and passively without requiring the control rods to be scrammed during a loss of coolant accident, incurring no core damage. Robust safety characteristics of the SCR-MFE-1500 are further enhanced during a postulated severe accident, including sabotage or any hostile actions, because of the capability of MFE for high-temperature containment of their fission product inventory (Ponamarev-Stepnoy et al., 1999). Due to the SiC ceramic coating, radioactivity would be kept intact within the MFEs. It is also very forgiving in that the MFE fuel element core would be protected from reactivity accidents resulting from the introduction of positive reactivity insertions. Any excess reactivity period that is not shorter than the MFE thermal delay time would be passively compensated due to negative reactivity coefficients for coolant/moderator water heating and evaporation. Only the core with MFE that is directly cooled by the coolant/moderator would possess such a unique feature of this self-protection (intrinsic safety). For MFE, the multiple coating of the fuel kernel performs the role of cladding. The acceptable temperature during severe accidents is ∼1500 °C (as proven by experiments).

5. Containment

The SC-MFE limiting conditions for the containment design are estimated to be less severe than for the

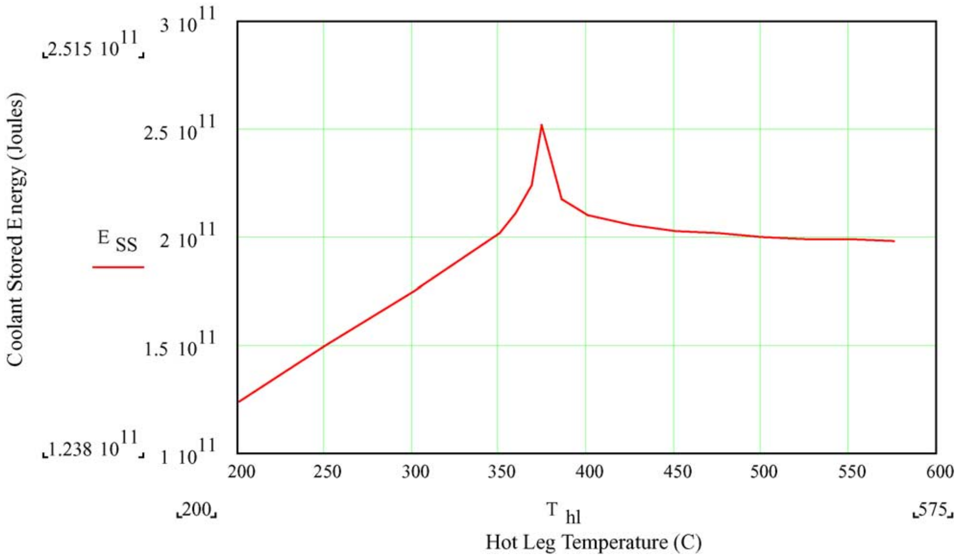

Fig. 5. SC-MFE coolant stored energy.

ABWR and CE +80, and comparable to the AP600. This is based on a comparison of the stored energy of the primary loop within containment, the initial rate of energy release for a large break LOCA, and the reactor total power (decay heat).

The maximum stored energy of the SC-MFE coolant occurs during startup when the system passes through the critical pressure/temperature, and not at full power. This is due to the decrease in hot leg density as reactor outlet temperature is increased from the critical temperature to the operating temperature of 550 °C. SC-MFE startup is assumed to be with sliding pressure control during power ascension based on the work done by Oka and Koshizuka (ABWR, 1996). Fig. 5 illustrates the coolant stored energy versus hot leg temperature for the SC-MFE. Note that startup stability is not addressed here. Additional work is required for the selection of an actual startup sequence. However, the assumed sequence adequately defines the stored energy within containment for this comparison.

The primary coolant loop volume within containment for the SC-MFE is estimated to be 350 m^3. Estimated total coolant stored energy is compared to the ABWR, AP600 and CE +80 in Table 2. This stored energy contains the energy of coolant that would not flash to steam following a LOCA. With its higher fluid enthalpy, the SC-MFE coolant will flash a higher percentage of mass to vapor. Available flash energy is estimated by assuming a final equilibrium state at 1 atm. The effective release energy (flash energy) is also compared. Although the SC-MFE operates at higher fluid enthalpy, the flash energy of the coolant is comparable to that of the AP600 and significantly less than the ABWR and CE +80. At full power, the SC-MFE stored and flash energies are reduced to 1.9 and 1.7×10^{11} J.

The initial rate of energy release for a LBLOCA is also estimated to be less for the SC-MFE, primarily due to the smaller cold leg and hot leg piping diameters (Table 2). The SC-MFE feedwater flow rate is ∼20% less than the ABWR, and several times less per loop than for the PWR reactors. The lower flow rate allows for a decrease in required pipe diameter that would compensate for the higher initial choke velocity and enthalpy associated with the SC-MFE fluid conditions. Also, the highest coolant stored energy occurs during reactor startup (∼20% more than at full power), which reduces the impact of decay heat during the peak energy release. Thus, the initial mass and energy release rates for a SC-MFE LOCA will be comparable to or less than these designs.

The intermediate and long-term energy release rates are also estimated to be less severe as the reactor piping and fuel stored thermal energy would be less. The pipe and vessel walls will have significantly less mass

Table 2
Comparison of SC-MFE key containment parameters

Parameters	SC-MFE	ABWR	AP600	CE +80
Thermal power (MW_t)	3390	3926	1933	3914
PCL volume (m^3)	350	700[a]	250[a]	400[a]
Coolant stored energy ($\times 10^{11}$ J)	2.5	3.8	2.3	4.0
Flash energy to 1 atm ($\times 10^{11}$ J)	2.2	3.0	1.8	3.2
Inlet/feedwater flow (10^6 kg/h)	6.04	7.62	33.7	75.2
Cold leg ID (cm)	2 at 49.0[b]	2 at 55.0	4 at 55.9	4 at 76.2
Hot leg ID (cm)	4 at 44.0	4 at 70.0 4 at 35.5[c]	2 at 78.7	2 at 106.7
Core average fuel temperature (°C)	550–600		650–750	
Zircaloy mass in core (kg)	–	>40000	16127	33565
Containment free volume (m^3)	TBD	13310	49270	95625

[a] Estimated from SAR reports Kotelnikov (1978), Oka and Koshizuka (2001) and AP600 (1992).
[b] The cold leg will split into four smaller diameter pipes at the vessel inlet.
[c] The ABWR uses a nozzle flow venturi to limit steam line break release rates.

inventory than for the PWR designs (no steam generators), and slightly less than for the ABWR design (smaller vessel). The core average fuel temperature is also significantly less for the SC-MFE due to the relatively large fuel surface area. Although decay heat would be higher than the AP600, it would be lower than the ABWR and CE +80. In addition, the SC-MFE concerns for hydrogen generation will be less severe as the fuel cladding does not contain Zr.

This simple comparison indicates that although the SC-MFE would operate in the supercritical steam region, limiting conditions imposed upon the containment design would be comparable to or less than existing advanced reactor designs. Detailed studies of the potential containment response are still needed, and life cycle cost assessments necessary to allow selection of a containment design (large or small, passive or active, etc.). However, of importance to the SC-MFE design is that the supercritical operating conditions do not appear to dictate a particular containment design and existing containment technologies can be used.

6. Fuel fabrication

Fuel assemblies with the bulk load of MFE, in fact, represent a symbiosis between the traditional PWR and BWR fuel elements with fuel pellets and the HTGR with spherical fuel elements. The following provides a comparative analysis of the fabrication costs and technologies.

It is known that the cost of zirconium cladding comprises 50% of the total fuel fabrication cost for PWR or BWR. Additionally, it should be noted that manual operations are nearly absent in MFE fabrication as the process is fully automatic, while for the traditional fuel, the amount of manual labor is rather high, in particular during the assembly and quality control activities. Manufacture of fuel rods with pellets implies the combination of various process steps, including assembling, welding, precise machining with small tolerances, filling with helium, application of coatings, several stages of quality control, etc. All these processes require appropriate equipment. It should also be noted that fabrication of fuel pellets consists of a number of steps—compaction, sintering, grinding, examination, rejection, reprocessing, etc. The modern line to assemble fuel rods from the readymade tubes, pellets, fittings and plugs consists of approximately 40 machines (22 process machines, 7 for inspection and 11 for handling). The analysis shows that the cost of MFE fabrication is comparable with the cost of just the pellets for a VVER or BWR (Tsiklauri et al., 2002).

In MFE fabrication, the application of coatings in the fluidized bed can be made fully automatic with the pre-set program of gases supply and MFE discharge. There is no grinding of the fuel kernel in MFE fabrication, which improves the economy of the process. For a standard LWR fuel pellet, there is a specific pellet grinding operation to meet the strict requirements of size and fuel-cladding clearance. The cost of pellet grinding is about 10% of the total fuel cost. Half of it is due to the damage of pellets during machining, the other half due to the reprocessing of wastes and associated consumption of fission materials.

The tests on tightness of the fresh fabricated MFE were performed using a weak irradiation method (Ponamarev-Stepnoy et al., 1983). This method is based on the irradiation of MFE in a reactor with a subsequent short time annealing to detect ^{135}Xe leakage and determine other fission products leakage. The control of SiC layer integrity was performed by annealing of particles and weighting them in the course of the tests. Also, chemical control methods were used. The results of many tests show that a tightness failure was very low (10^{-6}).

According to Kotelnikov, the fabrication cost of micro-fuel for the “DRAGON” reactor comprises 23.5% of the fuel element assembly (Tsiklauri et al., 2002). This means that the MFE for LWR with kernel diameter of 1.5 mm and total diameter of 1.8 mm should be four times cheaper than the fabrication of fuel for a HTRG (kernel diameter 0.5 mm, total diameter 1.0 mm) due to the specific volume of the coatings (total volume of coatings/fuel volume). In this way, technological and economic characteristics of the MFE for light water reactors have considerable margins as compared with HTRG.

Total weight of the fuel element skeleton shell for a VVER-1000 is about 150 kg and comprises 5% of the total fuel element cost. Preliminary studies show that the weight of the metal in the fuel element with MFE will not differ significantly from the traditional, i.e. the skeletal cost should be approximately the same as for the VVER-1000.

7. Fuel corrosion

VNIIAM and RRC Kurchatov Institute have performed experimental investigations of the impact produced by water and steam environments upon the SiC and PyC pellet coatings, specifically with regard to corrosion resistance. Long-term corrosion-resistance tests of MFE in water were performed at 350 °C and 190 bar over the course of 17.5 months. The tests in superheated steam were performed at 550°C and 100 bar over the course of up to 14.5 months. Also, short-term corrosion resistance tests of MFE in superheated steam were performed at 650–1000 °C under 1–50 bar over a time period varying from 20 min to 2 weeks. All samples maintained their integrity, and mass loss was practically zero (Filippov et al., 2003; Ponamarev-Stepnoy et al., 1999).

8. Cycle efficiency

A representative steam cycle design and heat balance was created for the SC-MFE (Fig. 6). The GateCycle™ computer code was used to develop the heat balance and system design. The net cycle generator output was estimated to be 1520 MW_e with a heat rate of 7624 Btu/kWh and overall efficiency of 44.75%. Gross generator output is estimated at 1534 MW_e. The net output includes turbine and generator efficiency losses, turbine mechanical losses, and all major pump power demands. The condensate booster pump (to 90 bar) and main feedwater pump (to 250 bar) were provided with steam turbines (modeled explicitly), using steam at the crossover pressure to the LPT. All other pumps were assumed to be electric motor driven. Not included in the net output estimate are turbine shaft gland seal steam, coolant blowdown and other minor loads.

The cycle design was patterned after a typical PWR/BWR steam cycle for the intermediate pressure turbine (IPT) and low pressure turbine (LPT), with a high pressure turbine (HPT) added for the front end supercritical steam. The IPT and LPT are effectively similar in size to a 1000 MW_e nuclear facility. The base design assumed a feedwater temperature and pressure of 300 °C and 250 bar, and a reactor power of 3390 MW_t. Supercritical steam conditions at the HPT inlet were 550 °C and 240 bar. The crossover pressure between the HPT and IPT was assumed to be 60 bar and 12.5 bar between the IPT and LPT. Moisture separation is assumed after the IPT exhaust, however, no reheat is assumed.

The HPT and IPT were assumed to have single flow ends and one extraction port each. The HPT was also assumed to use partial arcing with four inlet flow valves and two rows in the governing stage. The LPT was assumed to have dual flow ends and five extraction ports, with only the last three extraction ports designed for moisture removal. The GateCycle™ code (v 5.34) did not have built in moisture extraction curves for large nuclear turbines, and so macros were defined to calculate the moisture removal. Because of this, the LPT

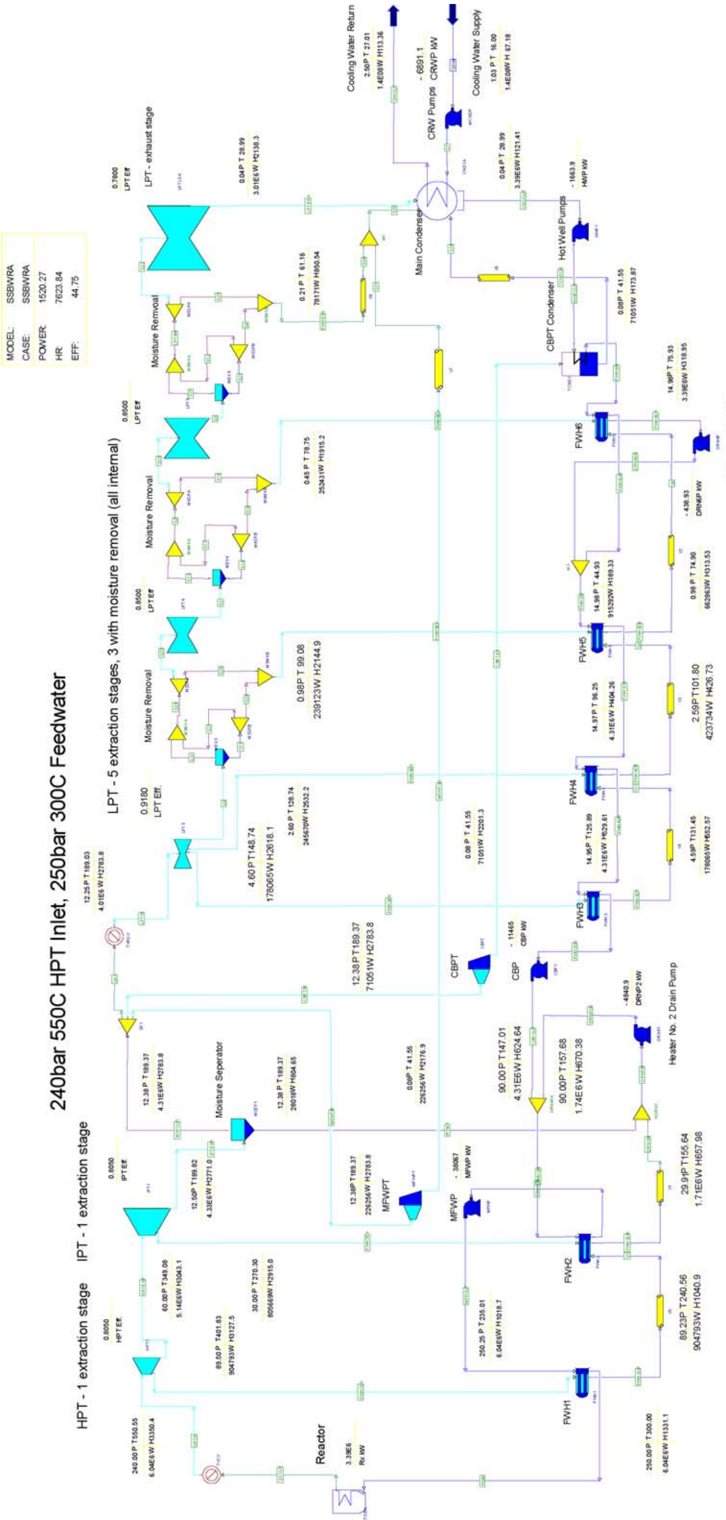

Fig. 6. SC-MFE design case (3390 MW_t h).

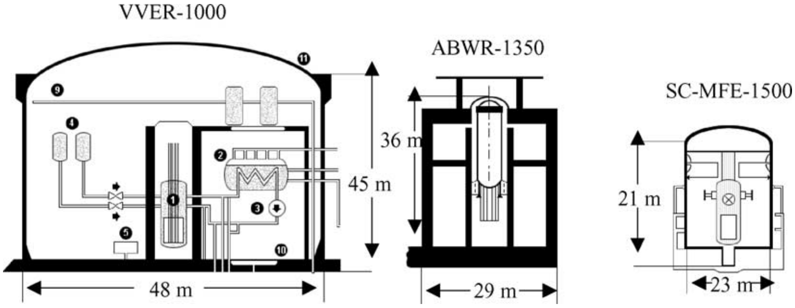

Fig. 7. Comparison of the size of containments for SC-MFE-1500, ABWR-1350 and VVER-1000.

moisture extraction stages were modeled explicitly, Fig. 6. In addition, the LPT is expected to consist of three parallel turbines but is lumped as a single turbine in the model.

The condensate booster pump turbine (CBPT) was configured with a separate condenser for heat recovery. However, the main feedwater pump turbine (MFWPT) is estimated to have too great a heat load to condense all of the exhaust steam with the condensate return (feedwater), and so this steam is returned to the main condenser. Six of the seven turbine extraction ports were configured with feedwater heaters (FWH). Each of the six FWHs were designed for a terminal temperature difference of 2.78 °C (5 °F) and a drain cooler approach temperature of 5.56 °C (10 °F). The seventh (last) extraction port of the LPT was assumed dumped directly to the main condenser, as the fluid temperature would be too low for use.

9. Capital cost

Potential economic improvement is understood by comparing plant sizes. The reactor plant building and containment for a SCR-MFE-1500 compared with the ABWR and a pressurized water reactor VVER-1000 are shown in Fig. 7. The improvement from the ABWR-1350 MW_e and VVER-1000 are obvious. The reactor pressure vessel is smaller in dimensions. For SCR-MFE-1500, the inside diameter is 5–6 m, for the ABWR-1350, the diameter is 7.1 m. Due to the elimination of steam separators, dryers and internal pumps for the once-through concept of the SCR-MFE-1500, the height of the vessel is 12.5 m. The ABWR height is 21.0 m. The thermal efficiency of the SCR-MFE-1500 is greatly improved compared with the ABWRs 28%. The required containment volume is reduced because the smaller reactor pressure vessel contains less coolant mass and less total coolant enthalpy. If a suppression pool design is used for the SCR-MFE-1500, the size of the containment can be reduced to 21 m × 23 m, with a volume of 8700 m^3. The ABWR has a containment vessel of approximately 25,000 m^3 (total). The containment expense is reduced significantly. The size of the steam turbine is reduced due to the reduced steam flow through the turbine, and no reheater is needed. The potential cost reduction in both reactor and turbines are the characteristics of the SCR concept. It should be noted that the SCR is the smallest reactor in size; however, the reactor power is higher than the ABWR-1350. At the present stage, it is difficult to calculate the economic benefits in the capital cost of the supercritical nuclear power plant compared with the ABWR-1350 and the VVER (PWR), although it can be predicted that the capital cost per installed kW_e is 30% less than for the ABWR-1350, and 40% less than for VVER-1000. Following the expert estimations, the capital cost for SCR-MFE-1500 will be less than US$ 1000/kW installed.

The operating cost for SCR-MFE plant is considerably less than for standard BWR due to a higher capacity factor and lower volume of waste production. Spent fuel pebbles pass continually into a storage tank, which will be designed to hold the spent fuel discharged during the plant's lifetime. Better availability factor, a lower investment into the construction of the plant due to the reduction and simplification of safety systems and many other technical and economic factors lead to a superior designed plant.

10. Conclusion

The supercritical pressure light water reactor with MFE is a safe and efficient technology for generation IV nuclear power plants. Designing and building of a NPP with the SCR-LWR-MFE is probably easier than that of a HTGR, because it is based on extensive experience of the industry with LWRs and worldwide acceptance and safe operation of the supercritical fossil fuel steam turbines.

References

ABWR Standard Safety Analysis Report. GE Nuclear Energy, August 1996.

AP600 Standard Safety Analysis Report. Westinghouse Electric Corp., June 1992.

Filippov, G., Bogojavlensky, R., Tsiklauri, G., Meriwether, G., 2003. Supercritical boiling water reactor concept with micro-fuel-elements. In: ICAAP'03, Cordoba, Spain.

Lee, J.H., Oka, Y., Koshizuka, S., 1999. Reliability Eng. Syst. Saf. 64, 327–338.

Kotelnikov, R., 1978. High Temperature Nuclear Fuel. Atomizdat, Moscow.

Oka, Y., Koshizuka, S., 2001. Supercritical-pressure, once-through cycle light water cooled reactor concept. J. Nucl. Sci. Technol. 38 (December (12)), 1081–1089.

Oka, Y., Koshizuka, S., Ishiwatari, Y., Yamaji, A., 2003. Conceptual design of high temperature reactor cooled by supercritical light water. In: ICAAP'03, Cordoba, Spain.

Ponamarev-Stepnoy, N., Khrulev, A., Mamot, V., 1983. Fuel elements of gas-cooled reactors and fuel reprocessing, Proceedings of IAEA Meeting, vol. 1, Moscow; Kukharkin, N., Filippov, G., Grishanin, E., et al. At. Energy, 86 (6) 261–270.

Ponamarev-Stepnoy, N., Kukharkin, N., Filippov, G., et al., 1999. Application of micro-fuel elements at light water reactors. At. Energy 86 (6).

Tsiklauri, G., Newman, D., Omberg, R., et al., 2002. Nucl. Plant J. 20 (1).